Inorg. Chem. **2007**, *46*, 7362–7370

Diverse Entangled Metal–Organic Framework Materials Incorporating Kinked Organodiimine and Flexible Aliphatic Dicarboxylate Ligands: Synthesis, Structure, Physical Properties, and Reversible Structural Reorganization

Matthew R. Montney,[†] Subhashree Mallika Krishnan,[†] Ronald M. Supkowski,[‡] and Robert L. LaDuca*[,†]

Lyman Briggs College and Department of Chemistry, Michigan State University, East Lansing, Michigan 48825, and Department of Chemistry and Physics, King's College, Wilkes-Barre, Pennsylvania 18711

Received February 13, 2007

Hydrothermal synthesis has afforded a family of divalent metal adipate (adp) coordination polymers incorporating the kinked dipodal organodiimine 4,4′-dipyridylamine (dpa). As revealed by single-crystal X-ray diffraction, the structures of these materials are critically dependent on the metal coordination geometry, the carboxylate binding modes, and the conformations of the flexible adipate moieties. In all cases, hydrogen-bonding interactions imparted by the dpa tethers also play a structure-directing role. All materials were further characterized via infrared spectroscopy and elemental and thermogravimetric analysis. [Co(adp)(dpa)] (**1**) displays doubly interpenetrated three-dimensional (3-D) networks with a decorated α-Po-type (pcu) topology. In contrast, [Ni(adp)(dpa)(H_2O)] (**2**) possesses a triply interpenetrated binodal cooperite-type (pts) framework, the highest level of interpenetration yet reported for this structure type. [Zn(adp)(dpa)]·H_2O (**3**) presents mutually inclined polycatenated 2-D graphitic layers consisting of neutral dimeric [$Zn_2(\mu_2$-adp)$_2$] kernels conjoined by dipodal dpa ligands. Compound **1** exhibited weak antiferromagnetic coupling between its carboxylate-bridged Co atoms, following Curie–Weiss behavior with $\Theta = -3.3$ K. Compound **3** manifested blue light emission under ultraviolet excitation, as well as a reversible structural reorganization upon dehydration/rehydration.

Introduction

Interest remains high in functional metal−organic framework materials (MOFs) because of their capabilities in hydrogen storage,[1] shape-selective separations,[2] ion-exchange,[3] catalysis,[4] and optical properties.[5−7] In the construction of these materials, benzenedicarboxylate and benzenetricarboxylate ligands are frequently employed to connect cationic metal nodes, providing the necessary charge balance to permit construction of a wide variety of neutral frameworks without incorporation of smaller anions that could

* To whom correspondence should be addressed. Mailing address: Lyman Briggs College, E-30 Holmes Hall, Michigan State University, East Lansing, Michigan 48825. E-mail: laduca@msu.edu.

† Michigan State University.

‡ King's College.

(1) For example, see: (a) Li, H.; Eddaoudi, M.; O'Keeffe, M.; Yaghi, O. M. *Nature* **2005**, *402*, 276−279. (b) Matsuda, R.; Kitaura, R.; Kitagawa, S.; Kubota, Y.; Belosludov, R. U.; Kobayashi, T. C.; Sakamoto, H.; Chiba, T.; Takata, M., Kawazoe, Y.; Mita, Y. *Nature* **2005**, *436*, 238−241. (c) Pan, L.; Holson, D.; Ciemnolonski, L. R.; Heddy, R.; Li, J. *Angew. Chem., Int. Ed.* **2006**, *46*, 616−619. (d) Rosi, N. L.; Eckert, J.; Eddaoudi, M.; Vodak, D. J.; Kim, J.; O'Keeffe, M.; Yaghi, O. M. *Science* **2003**, *300*, 1127−1129. (e) Dinca, M.; Yu, A. F.; Long, J. R. *J. Am. Chem. Soc.* **2006**, *128*, 8904−8913. (f) Ferey, G.; Latroche, M.; Serre, C.; Millange, F.; Loiseau, T.; Percheron-Guegan, A. *Chem. Commun.* **2003**, 2976−2977. (g) Zhao, X.; Xiao, B.; Fletcher, A. J.; Thomas, K. M.; Bradshaw, D.; Rosseinsky, M. J. *Science* **2004**, *306*, 1012−1015. (h) Roswell, J. L. C.; Yaghi, O. M. *Agnew. Chem., Int. Ed.* **2005**, *44*, 4670−4679. (i) Kondo, M.; Okubo, T.; Asami, A.; Noro, S.-I.; Yoshitomi, T.; Kitagawa, S.; Ishii, T.; Matsuzaka, H. *Agnew. Chem., Int. Ed.* **1999**, *38*, 140−143. (j) Sudik, A. C.; Millward, A. R.; Ockwig, N. W.; Cote, A. P.; Kim, J.; Yaghi, O. M. *J. Am. Chem. Soc.* **2005**, *127*, 7110−7118.

(2) For example, see: (a) Seo, J. S.; Whang, D.; Lee, H.; Jun, S. I.; Oh, J.; Jeon, Y. J.; Kim, K. *Nature* **2000**, *404*, 982−986. (b) Cingolani, A.; Galli, S.; Masciocchi, N.; Pandolfo, L.; Pettinari, C.; Sironi, A. *J. Am. Chem. Soc.* **2005**, *127*, 6144−6145.

(3) For example, see: (a) Fang, Q.-R.; Zhu, G.-S.; Xue, M.; Sun, J.-Y.; Qiu, S.-L. *Dalton Trans.* **2006**, 2399−2402. (b) Zhang, X.-M.; Tong, M.-L.; Lee, H. K.; Chen, X.-M. *J. Solid State Chem.* **2001**, *160*, 118−122. (c) Yaghi, O. M.; Li, H.; Groy, T. L. *Inorg. Chem.* **1997**, *36*, 4292−4293.

(4) For example, see: (a) Guillou, N.; Forster, P. M.; Gao, Q.; Chang, J. S.; Nogues, M.; Park, S.-E.; Cheetham, A. K.; Ferey, G. *Angew. Chem., Int. Ed.* **2001**, *40*, 2831−2834. (b) Wu, C.-D.; Hu, A.; Zhang, L.; Lin, W. *J. Am. Chem. Soc.* **2005**, *127*, 8940−8941. (c) Han, H.; Zhang, S.; Hou, H.; Fan, Y.; Zhu, Y. *Eur. J. Inorg. Chem.* **2006**, *8*, 1594−1600. (d) Mori, W.; Takamizawa, S.; Kato, C. N.; Ohmura, T.; Sato, T. *Microporous Mesoporous Mater.* **2004**, *73*, 15−30. (e) Baca, S. G.; Reetz, M. T.; Goddard, R.; Filippova, I. G.; Simonov, Y. A.; Gdaniec, M.; Gerbeleu, N. *Polyhedron* **2006**, *25*, 1215−1222.

10.1021/ic070291d CCC: $37.00 © 2007 American Chemical Society
Published on Web 08/10/2007

inhibit formation of void spaces. An extremely diverse range of structural motifs occur in these systems, predicated on the disposition of the donor atoms within the organic component and metal coordination preferences. The level of structural complexity in benzenecarboxylate MOFs has been enhanced through incorporation of neutral nitrogen-donor-tethering ligands such as 4,4′-bipyridine (4,4′-bpy), which can connect metal cations through its distal pyridyl nitrogen donor atoms into structurally intriguing solids with potentially useful properties.[6−8] For example, the paratactic layered phase {[Zn(isophthalate)(4,4′-bpy)$_2$][Zn(isophthalate)-(4,4′-bpy)]·0.25H$_2$O exhibits blue luminescence upon ultraviolet irradiation,[7] and the interpenetrated 3-D material [Zn(terephthalate)(4,4′-bpy)$_{0.5}$] can chromatographically separate branched and linear hydrocarbons.[8]

Compared with benzenedicarboxylate MOFs, organodiimine-scaffolded coordination polymers based on longer aliphatic α,ω-dicarboxylates have received less attention.[9−14] While the structural rigidity of benzenedicarboxylate subunits can prove advantageous for the construction of porous materials, flexible aliphatic dicarboxylates can provoke novel structural motifs because of their ability to access numerous energetically similar conformations. For instance, a few divalent metal adipate (adp) coordination polymers incorporating 4,4′-bpy or 1,2-di-4-pyridylethane (bpe) have been reported, in many cases, manifesting doubly interpenetrated 3-D networks.[9−11,14]

For some time we have been interested in the synthesis and characterization of coordination polymers containing the organodiimine 4,4′-dipyridylamine (dpa). Unlike 4,4′-bpy, dpa possesses a kinked disposition of its terminal nitrogen donor atoms, as well as a hydrogen-bonding locus at its center, allowing it to promote the formation of novel structural patterns via supramolecular and covalent interactions. The combination of dpa with appropriate metal precursors under hydrothermal conditions has resulted in the construction of extended solids with diverse structural motifs.[15−17] For example, {[Ni(dpa)$_2$(succinate)$_{0.5}$]Cl} exhibits a unique 5-connected self-penetrated structure with a uniform 6^{10} topology.[15] [CuMoO$_4$(dpa)$_2$]·2H$_2$O possesses 2-D copper molybdate lamella strutted by dpa tethers, which in turn, anchor waters of crystallization in incipient voids via N−H···O hydrogen bonding.[16] [Mo$_4$O$_{13}$(dpaH)$_2$] displays hydrogen-bonded interdigitated 1-D molybdate chains and is able to intercalate primary and secondary amines.[17] Herein, we report the hydrothermal synthesis and characterization of divalent cobalt, nickel, and zinc dpa-tethered metal adipate interpenetrated or polycatenated coordination polymers. In this class of materials, metal coordination geometry, carboxylate binding mode, conformational flexibility of the adipate subunits and dpa-promoted supramolecular interactions appear to play a synergistic role in structure direction. Preliminary physical property studies (thermal degradation, magnetism, and luminescence) were also undertaken to gauge the functional potential of this family of materials. The zinc derivative also undergoes a reversible structural reorganization upon dehydration and rehydration.

Experimental Section

General Considerations. CoCl$_2$·6H$_2$O, NiCl$_2$·6H$_2$O, ZnCl$_2$ (Fisher), and adipic acid (Aldrich) were obtained commercially. 4,4′-Dipyridylamine (dpa) was prepared via a published procedure.[17] Water was deionized above 3 MΩ in-house. Thermogravimetric analysis was performed on a TA Instruments TGA 2050 thermogravimetric analyzer with a heating rate of 10 °C min^{-1} up to 900 °C. Elemental analysis was carried out using a Perkin-Elmer 2400 Series II CHNS/O analyzer. IR spectra were recorded on a Mattson Galaxy FTIR Series 3000 using KBr pellets. Powder X-ray diffraction patterns were obtained via Θ−2Θ scans performed on a Rigaku Rotaflex instrument. Variable-temperature magnetic susceptibility data (2−300 K) was collected on a Quantum Design MPMS SQUID magnetometer at an applied field of 0.1 T. After each temperature change, the sample was kept at the new temperature for 5 min before magnetization measurement to ensure thermal equilibrium. The susceptibility data was corrected for diamagnetism using Pascal's constants.[18] Luminescence spectra were obtained with a Hitachi F-4500 fluorescence spectrometer on solid crystalline samples anchored to quartz microscope slides with Rexon Corporation RX-22P ultraviolet-transparent epoxy adhesive.

Preparation of [Co(adp)(dpa)] (1). CoCl$_2$·6H$_2$O (88 mg, 0.37 mmol), dpa (127 mg, 0.73 mmol), and adipic acid (54 mg, 0.37 mmol) were placed into 10 mL of distilled H$_2$O in a 23 mL Teflon-lined Parr acid digestion bomb. The bomb was sealed and heated at 120 °C for 44 h, whereupon it was cooled slowly to 25 °C. Magenta blocks of **1** (83 mg, 60% yield based on Co) were isolated after washing with distilled water, ethanol, and acetone

(5) For example, see: (a) Zang, S.; Su, Y.; Li, Y.; Ni, Z.; Meng, Q. *Inorg. Chem.* **2006**, *45*, 174−180. (b) Wang, L.; Yang, M.; Li, G.; Shi, Z.; Feng, S. *Inorg. Chem.* **2006**, *45*, 2474−2478. (c) Wang, S.; Hou, Y.; Wang, E.; Li, Y.; Xu, L.; Peng, J.; Liu, S.; Hu, C. *New J. Chem.* **2003**, *27*, 1144−1147. (d) Beauvais, L. G.; Shores, M. P.; Long, J. R. *J. Am. Chem. Soc.* **2000**, *122*, 2763−2772. (e) Jianghua, H.; Jihong, Y.; Yuetao, Z.; Qinhe, P.; Ruren, X. *Inorg. Chem.* **2005**, *44*, 9279−9282.

(6) For example, see: (a) Lu, W.-G.; Su, C.-Y.; Lu, T.-B.; Jiang, L.; Chen, J.-M. *J. Am. Chem. Soc.* **2006**, *128*, 34−35. (b) Horike, S.; Matsuda, R.; Kitagawa, S. *Stud. Surf. Sci. Catal.* **2005**, *156*, 725−732. (c) Qin, C.; Wang, X.-L.; Li, Y.-G., Wang, E.-B.; Su, Z.-M.; Xu, L., Clerac, R. *Dalton Trans.* **2005**, 2609−2614. (d) Zheng, Y.-Q.; Ying, E.-R. *Polyhedron* **2005**, *24*, 397−406. (e) Ghosh, S. K.; Ribas, J.; Bharadwaj, P. K. *Crystal Growth Des.* **2005**, *5*, 623−629. (f) Sun, X.-Z.; Sun, Y.-F.; Ye, B.-H.; Chen, X.-M. *Inorg. Chem. Commun.* **2003**, *6*, 1412−1414.

(7) Dai, Y.-M.; Ma, E.; Tang, E.; Zhang, J.; Li, J.-Z.; Huang, X.-D.; Yao, Y.-G. *Crystal Growth Des.* **2005**, *5*, 1313−1315.

(8) Chen, B.; Liang, C.; Yang, J.; Contreras, D. S.; Clancy, Y. L.; Lobkovsky, E. B.; Yaghi, O. M.; Dai, S. *Angew. Chem., Int. Ed.* **2006**, *45*, 1390−1393.

(9) Long, L.-S.; Wu, Y.-R.; Huang, R.-B.; Zheng, L.-S. *Inorg. Chem.* **2004**, *43*, 3798−3800.

(10) Hu, R.-F.; Kang, Y.; Zhang, J.; Li, Z.-J.; Qin, Y.-Y.; Yao, Y.-G. *Z. Anorg. Allg. Chem.* **2005**, *631*, 3053−3057.

(11) Zheng, Y.-Q.; Lin, J.-L.; Kong, Z.-P. *Inorg. Chem.* **2004**, *43*, 2590−2596.

(12) Liao, J.-H.; Cheng, S.-H.; Tsai, H.-L.; Yang, C.-I. *Inorg. Chim. Acta* **2002**, *338*, 1−6.

(13) Hao, N.; Shen, E.; Wang, Y.-E.; Hu, C.-W.; Xu, L. *Eur. J. Inorg. Chem.* **2004**, 4102−4107.

(14) Mukherjee, P. S.; Konar, S.; Zangrando, E.; Mallah, T.; Ribas, J.; Chaudhuri, N. R. *Inorg. Chem.* **2003**, *42*, 2695−2703.

(15) Montney, M. R.; Mallika Krishnan, S.; Patel, N. M.; Supkowski, R. M.; LaDuca, R. L. *Crystal Growth Des.* **2007**, *7*, 1145−1153.

(16) Hagrman, D.; Warren, C. J.; Haushalter, R. C.; Seip, C.; O'Connor, C. J.; Rarig, R. S.; Johnson, K. M.; LaDuca, R. L.; Zubieta, J. *Chem. Mater.* **1998**, *10*, 3294−3297.

(17) Zapf, P. J.; LaDuca, R. L.; Rarig, R. S.; Johnson, K. M.; Zubieta, J. *Inorg. Chem.* **1998**, *37*, 3411−3414.

(18) Khan, O. *Molecular Magnetism*; VCH Publishers: New York, 1993.

and drying in air. Anal. Calcd for $C_{16}H_{17}CoN_3O_4$ (**1**): C, 51.35; H, 4.58; N, 11.23%. Found: C, 51.09; H, 4.24; N, 11.11%. IR (KBr, cm^{-1}): 3450 s br, 3302 s, 3180 s, 3075 m, 2937 s, 2858 s, 1650 m, 1596 s, 1531 s, 1500 m, 1443 m, 1408 m, 1366 m, 1322 m, 1305 m, 1209 m, 1146 w, 1098 w, 1066 w, 1053 w, 1018 m, 975 w, 944 w, 926 w, 910 w, 857 w, 822 m, 780 w, 732 w, 681 w, 629 w, 591 w, 535 w.

Preparation of [Ni(adp)(dpa)(H_2O)] (2). $NiCl_2 \cdot 6H_2O$ (88 mg, 0.37 mmol), dpa (127 mg, 0.73 mmol), and adipic acid (54 mg, 0.37 mmol) were placed into 10 mL of distilled H_2O in a 23 mL Teflon-lined Parr acid digestion bomb. The bomb was sealed and heated at 120 °C for 44 h, whereupon it was cooled slowly to 25 °C. Green blocks of **2** (91 mg, 63% yield based on Ni) were isolated after washing with distilled water, ethanol, and acetone and drying in air. Anal. Calcd for $C_{16}H_{19}NiN_3O_5$ (**2**): C, 49.02; H, 4.89; N, 10.72%. Found: C, 48.67; H, 4.66; N, 10.56%. IR (KBr, cm^{-1}): 3430 m, 3296 m, 3181 m, 3135 m, 3093 m, 3048 m, 2960 m, 2917 m, 2895 m, 1633 m, 1604 s, 1527 s, 1487 s, 1412 s, 1347 s, 1307 m, 1293 m, 1232 w, 1217 s, 1160 m, 1103 w, 1075 w, 1060 w, 1022 m, 977 w, 936 w, 899 w, 879 w, 815 m, 777 m, 727 w, 695 w, 680 w, 663 w, 641 w, 620 w, 596 m, 543 m, 467 w.

Preparation of {[Zn(adp)(dpa)]·H_2O} (3). $ZnCl_2$ (50 mg, 0.37 mmol), dpa (127 mg, 0.73 mmol), and adipic acid (54 mg, 0.37 mmol) were placed into 10 mL of distilled H_2O in a 23 mL Teflon-lined Parr acid digestion bomb. The bomb was sealed and heated at 120 °C for 96 h, whereupon it was cooled slowly to 25 °C. Colorless blocks of **3** (97 mg, 66% yield based on Zn) were isolated, after washing with distilled water, ethanol, and acetone and drying in air. Anal. Calcd for $C_{16}H_{19}N_3O_5Zn$ (**3**): C, 48.20; H, 4.80; N, 10.54%. Found: C, 47.91; H, 4.67; N, 10.52%. IR (KBr, cm^{-1}): 3376 s br, 3309 m, 2973 m, 2928 m, 2859 m, 1716 w, 1698 w, 1683 w, 1600 s br, 1522 s, 1490 m, 1445 m, 1429 m, 1408 m, 1351 s, 1317 m, 1278 w, 1209 m, 1152 m, 1062 m, 1000 s, 874 m, 855 w, 818 m, 741 w, 729 w, 645 m, 603 m, 537 m, 528 w.

X-ray Crystallography. A magenta block of **1** (0.20 mm × 0.16 mm × 0.16 mm), a light green prism of **2** (with dimensions 0.28 mm × 0.22 mm × 0.20 mm), and a colorless rhomb of **3** (0.35 mm × 0.30 mm × 0.30 mm) were subjected to single-crystal X-ray diffraction using a Bruker-AXS SMART 1k CCD instrument. Reflection data was acquired using graphite-monochromated Mo Kα radiation (λ = 0.71073 Å). The data was integrated via SAINT.[19] Lorentz and polarization effect and empirical absorption corrections were applied with SADABS.[20] The structures were solved using direct methods and refined on F^2 using SHELXTL.[21] All non-hydrogen atoms were refined anisotropically. Hydrogen atoms bound to carbon atoms were placed in calculated positions and refined isotropically with a riding model. The hydrogen atoms bound to the central nitrogen of the dpa moieties and any water molecules in **1**−**3** were found via Fourier difference maps, then restrained at fixed positions and refined isotropically. Relevant crystallographic data for **1**−**3** is listed in Table 1; more detailed information is available in the respective CIF files (see Supporting Information).

Results and Discussion

Synthesis and Spectral Characterization. The coordination polymers **1**−**3** were prepared cleanly and in high yield as single-phase crystalline products under hydrothermal conditions via combination of the appropriate metal chloride, 4,4′-dipyridylamine, and adipic acid. The infrared spectra of **1**−**3** were fully consistent with their formulations. Sharp, medium intensity bands in the range of ∼1600−1200 cm^{-1} were ascribed to stretching modes of the pyridyl rings of the dpa moieties.[22] Features corresponding to pyridyl ring puckering mechanisms were evident in the region between 820 and 600 cm^{-1}. Asymmetric and symmetric C−O stretching modes of the adipate carboxylate moieties were evidenced by very strong, slightly broadened bands at ∼1600 and ∼1400 cm^{-1}. Broad bands in the region of ∼3400−3200 cm^{-1} in all cases represent N−H stretching modes within the dpa ligands and O−H stretching modes within either aquo ligands or water molecules of crystallization, where present. The broadness of these latter spectral features is caused by significant hydrogen-bonding pathways within **1**−**3**.

Table 1. Crystal and Structure Refinement Data for **1**−**3**

	1	**2**	**3**
empirical formula	$C_{16}H_{17}CoN_3O_4$	$C_{16}H_{19}N_3NiO_5$	$C_{16}H_{19}N_3O_5Zn$
fw	374.26	392.05	398.71
collection T (K)	173(2)	173(2)	293(2)
λ (Å)	0.71073	0.71073	0.71073
cryst syst	monoclinic	monoclinic	orthorhombic
space group	*C*2/*c*	*C*2/*c*	*Pbcn*
a (Å)	16.5935(18)	23.157(3)	21.472(5)
b (Å)	9.9693(11)	9.3556(13)	8.542(2)
c (Å)	19.166(2)	17.074(2)	18.807(5)
α (deg)	90	90	90
β (deg)	95.781(2)	119.455(2)	90
γ (deg)	90	90	90
V ($Å^3$)	3154.4(6)	3220.9(8)	3449.8(15)
Z	8	8	8
D_{calcd} (g cm^{-3})	1.576	1.617	1.535
μ (mm^{-1})	1.114	1.239	1.456
R1[a] (all data)	0.0771	0.0542	0.0792
wR2[b] (all data)	0.0862	0.0744	0.1034

[a] $R1 = \sum||F_o| - |F_c||/\sum|F_o|$. [b] $wR2 = \sum\{[w(F_o^2 - F_c^2)^2]/\sum[wF_o^2]^2\}^{1/2}$.

Structural Description of [Co(adp)(dpa)] (1). The asymmetric unit of **1** (Figure 1) possesses one Co atom, one dpa ligand with an interring torsion angle of 25.9°, and two halves of two different adipate moieties (A, denoted by atom sets C21−C23 and O1−O2; B, denoted by atom sets C31−C33 and O3−O4). Co is ligated by two cisoid oxygen donors (O1 and O2) from a single chelating carboxylate terminus of A, by two *cis*-disposed oxygen atoms (O3 and O4A) from two different B ligands, and by two *trans*-disposed nitrogen atoms belonging to two crystallographically identical dpa ligands. The Co atoms in **1** therefore manifest a distorted octahedral [*trans*-CoO_4N_2] coordination environment, with Co−N bond lengths ranging from 2.14 to 2.20 Å and Co−O bond lengths from 2.01 to 2.27 Å. The bond lengths between Co and the chelating carboxylate oxygen donors are markedly longer than those to the monodentate carboxylate oxygen atoms. The bond angles about Co range from ∼59° (the bite

(19) *SAINT, Software for Data Extraction and Reduction*, version 6.02; Bruker AXS, Inc.: Madison, WI, 2002.
(20) *SADABS, Software for Empirical Absorption Correction*, version 2.03; Bruker AXS, Inc.: Madison, WI, 2002.
(21) Sheldrick, G. M. *SHELXTL, Program for Crystal Structure Refinement*; University of Gottingen: Gottingen, Germany, 1997.
(22) Kurmoo, M.; Estournes, C.; Oka, Y.; Kumagai, H.; Inoue, K. *Inorg. Chem.* **2005**, *44*, 217−224.

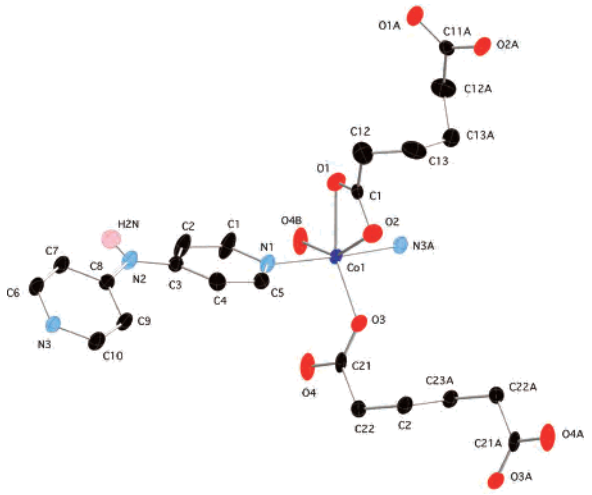

Figure 1. Expanded asymmetric unit of **1** with thermal ellipsoids at 50% probability. Most hydrogen atoms have been removed for clarity.

Table 2. Selected Bond Distances (Å) and Angles (deg) for **1**[a]

Co1−O4	2.024(2)	O4−Co1−O3$^{\#1}$	124.43(10)
Co1−O3$^{\#1}$	2.033(2)	O4−Co1−N3$^{\#2}$	84.85(9)
Co1−N3$^{\#2}$	2.155(2)	O3$^{\#1}$−Co1−N3$^{\#2}$	90.71(9)
Co1−O1	2.156(2)	O4−Co1−O1	93.33(9)
Co1−N1	2.175(2)	O3$^{\#1}$−Co1−O1	142.21(8)
Co1−O2	2.270(2)	N3$^{\#2}$−Co1−O1	91.21(9)
O1−C11	1.243(3)	O4−Co1−N1	90.29(8)
O2−C11	1.253(3)	O3$^{\#1}$−Co1−N1	93.68(9)
O4−C21	1.255(3)	N3$^{\#2}$−Co1−N1	174.75(9)
O3−C21	1.244(4)	O1−Co1−N1	87.08(9)
		O4−Co1−O2	151.92(9)
		O3$^{\#1}$−Co1−O2	83.53(8)
		N3$^{\#2}$−Co1−O2	93.03(9)
		O1−Co1−O2	58.67(8)
		N1−Co1−O2	90.32(9)
		O3−C21−O4	124.8(3)
		O1−C11−O2	120.8(3)

[a] Symmetry transformations to generate equivalent atoms: #1 $-x + 1/2$, $-y + 5/2$, $-z$; #2 $x + 1/2$, $-y + 5/2$, $z + 1/2$.

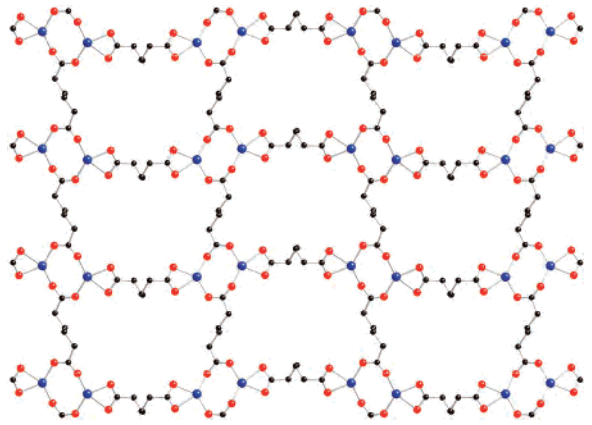

Figure 2. View down (1 0 1) of a neutral [$Co_2(\mu_2$-adp)(μ_4-adp)] layer in **1**.

angle of the chelating carboxylate unit in A) to ∼124°. Selected bond distances and angles for **1** are given in Table 2.

Extension of the structure through both type of adipate moieties along the (1 0 1) crystal plane results in a neutral [Co(adp)] layer (Figure 2) similar to those seen in the related 4,4′-bpy-containing phase [Mn(adp)(4,4′-bpy)].[11] Each Co

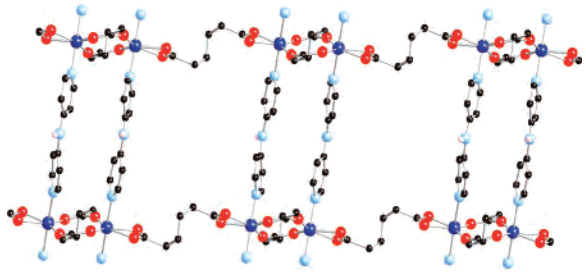

Figure 3. View down *b* of **1** illustrating cross-linking of two 2-D [Co_2-(μ_2-adp)(μ_4-adp)] layers through dpa tethering ligands.

atom connects to a neighboring Co atom via a bischelating bisbridging μ_2-adipate moiety (type A), with a through-ligand Co−Co distance of 9.448(1) Å. The bischelating adipate dianions rest in a very twisted gauche−gauche−gauche conformation (four-atom torsion angles = 59.8, 64.1, and 59.8°). Each Co atom further connects to five other Co atoms through two different exotetradentate μ_4-adipate ligands (type B), within which, each oxygen donor atom binds to cobalt in a monodentate fashion. Type B adipate moieties exist in an S-shaped conformation, with a gauche−anti−gauche pattern (four-atom torsion angles = 73.3, 180.0, and 73.3°). Dimeric kernels are built from the bridging of two nearest-neighbor Co atoms (Co−Co through-space distance of 3.966-(1) Å) through two carboxylate termini on two different B-type ligands, thereby forming 8-membered $(CoOCO)_2$ rings. Both carboxylate termini of B adipates bridge adjacent Co centers in a syn−syn conformation (Co−O···O−Co torsion angle = 26.9°). Within the layer motif, dimeric subunits linked by type B exotetradentate adipate anions tilt in the same direction, while those linked through A-type bisbridging adipate units tilt in the opposite direction. The [$Co_2(\mu_2$-adp)(μ_4-adp)] 2-D layers can be viewed as a system of conjoined 8-membered $(CoOCO)_2$ and 36-membered $(CoOC_6O)_4$ rings.

Each [$Co_2(\mu_2$-adp)(μ_4-adp)] layer connects to two other identical layers through tethering dpa struts, with an interlayer Co−Co distance of 12.063(1) Å, constructing a full covalent 3-D network with the general formulation [Co(adp)(dpa)], depicted in Figure 3. The covalent connectivity of the 3-D network is assisted by two types of supramolecular interaction, as revealed by PLATON.[23] Pyridyl rings belonging to neighboring dpa ligands engage in $\pi-\pi$ stacking interactions with a centroid-to-centroid distance of 3.997(2) Å and an interring dihedral angle of 7.6°. In addition, weak C−H···O interactions exist between the dpa moieties and carboxylate oxygen atoms of adipate ligand type B (C1···O4 = 2.925 Å, C10···O4 = 2.863 Å). If the 8-membered $(CoOCO)_2$ rings are taken as a single connecting node, the short topological symbol for the [Co(adp)(dpa)] coordination polymer network is $4^{12}6^3$, consistent with a 6-connected decorated α-Po (pcu)[24] net.

(23) Spek, A. L. *PLATON, A Multipurpose Crystallographic Tool*; Utrecht University: Utrecht, The Netherlands, 1998.

(24) The three-letter abbreviations for many common network topologies can be found in Delgado Friedrichs, O.; O'Keeffe, M.; Yaghi, O. M. *Acta Crystallogr.* **2003**, *A59*, 22−27. A useful searchable database of networks and tilings relevant to coordination polymer chemistry can be found on the Internet at http://rcsr.anu.edu.au/.

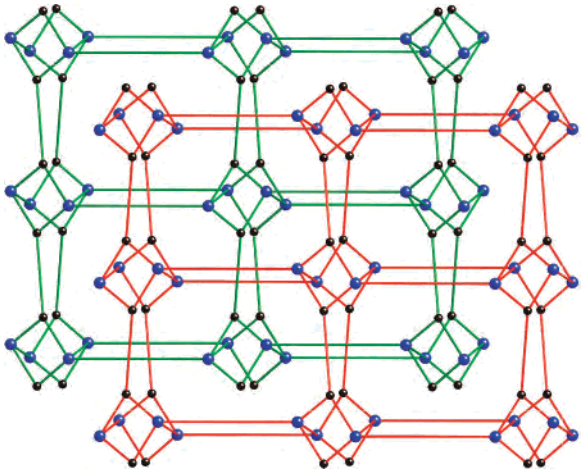

Figure 4. Framework perspective of **1** depicting its doubly interpenetrated decorated pcu-type 3-D network structure. Only Co and terminal C atoms of μ_4-adipate ligands are shown.

Table 3. Classical Hydrogen-Bonding Distances (Å) and Angles (deg) for **1**−**3**

D−H···A	*d*(H···A)	∠DHA	*d*(D···A)	symmetry transformation for A
		1		
N2−H2N···O1	1.879	172.50	2.738	$-x, -y+3, -z$
		2		
O5−H5A···O2	1.868	151.45	2.624	
O5−H5B···O3	1.994	175.89	2.825	$x, y-1, z$
N2−H2N···O4	2.013	172.00	2.855	$x-1/2, -y-3/2, z-1/2$
		3		
O1W−H1WA···O2	1.992	161.98	2.812	$x, y-1, z$
O1W−H1WB···O3	1.980	173.98	2.823	
N3−H3N···O1W	1.944	173.58	2.821	$x, -y, z-1/2$

The apparent void space within a single [Co(adp)(dpa)] pcu framework is occupied by an identical 3-D framework (Figure 4), with a full interpenetration vector (FIV)[25] in the (1/2, 1/2, 0) direction with a translation distance of 9.68 Å (calculated by TOPOS software[26]) in a fashion very similar to that of the previously reported [Mn(adp)(bpe)] phase.[14] The Class Ia (translation-only) double interpenetration[25] of the independent networks in **1** is assisted by interframework hydrogen bonding between the central N−H unit of the dpa moieties to ligated carboxylate oxygen atoms of type O1 belonging to bischelating type A adp ligands. Metrical parameters for these supramolecular interactions are listed in Table 3. No residual void space exists within the structure of **1**.

Structural Description of [Ni(adp)(dpa)(H_2O)] (2). The asymmetric unit of **2** (Figure 5) was revealed to contain two crystallographically distinct Ni atoms sited on inversion centers, one doubly deprotonated dianionic adipate, one neutral dpa ligand, and one aquo ligand bound to Ni2. Ni2 manifests [NiO_4N_2] octahedral coordination. The dpa nitrogen donors are oriented in a trans fashion at Ni2, as are the two symmetry-related aquo ligands. The two remaining trans coordination sites are occupied by oxygen donors from monodentate carboxylate subunits belonging to two symmetry-related adipate ligands. Ni1 possesses a distorted [NiO_4N_2] octahedral coordination sphere featuring two symmetry-related chelating adipate carboxylate subunits (with O−Ni−O bite angle of 61.5°) and two cis-disposed dpa nitrogen termini (N−Ni−N angle of 97.6°). The chelation of the adipate moiety is asymmetric, with each carboxylate subunit instigating one short (2.070 Å) and one long (2.196 Å) Ni−O bond. The deviation from an idealized octahedral coordination geometry at Ni1 can be ascribed to the requirements imposed by carboxylate chelation. The Ni2 to adipate oxygen bond distances (∼2.04 Å) are slightly shorter than those to Ni1, reflective of the monodentate carboxylate binding mode at Ni2. The trans-disposed nitrogen donors at Ni2 atoms have noticeably longer Ni−N distances (by ∼ 0.1 Å) than the cis-oriented dpa nitrogen atoms at Ni1, perhaps because of the more congested chelation-free coordination environment at Ni2. Selected bond data for **2** are given in Table 4.

Unlike in **1**, the adipate moieties in **2** serve only as exobidentate μ_2-bridging ligands. The adipate ligand has one carboxylate terminus chelating to Ni1, while the other end-capping carboxylate coordinates to Ni2 in a monodentate

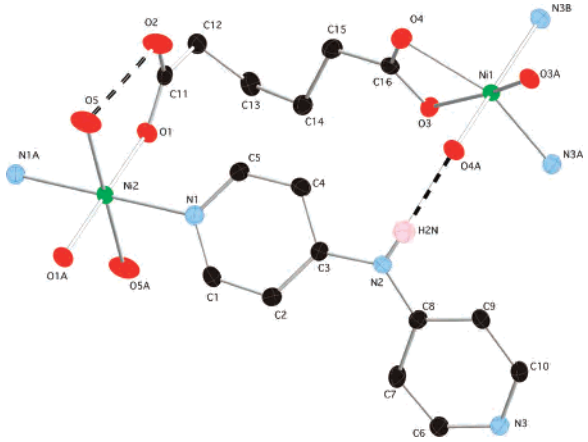

Figure 5. Expanded asymmetric unit of **2** with thermal ellipsoids at 50% probability. Most hydrogen atoms have been omitted for clarity. Hydrogen-bonding interactions are indicated as dashed lines.

Table 4. Selected Bond Distances (Å) and Angles (deg) for **2**[a]

Ni1−N3 (×2)	2.0313(17)	$N3^{\#3}$−Ni1−N3	97.71(10)
Ni1−$O3^{\#1,\#2}$ (×2)	2.0699(14)	N3−Ni1−$O3^{\#1}$	96.38(6)
Ni1−$O4^{\#1,\#2}$ (×2)	2.1956(15)	N3−Ni1−$O3^{\#2}$	94.15(6)
Ni2−O1 (×2)	2.0410(14)	$O3^{\#1}$−Ni1−$O3^{\#2}$	163.97(8)
Ni2−O5 (×2)	2.0502(15)	N3−Ni1−$O4^{\#1}$	91.61(6)
Ni2−N1 (×2)	2.1204(17)	$O3^{\#1}$−Ni1−$O4^{\#1}$	61.47(5)
O1−C11	1.264(2)	$O3^{\#2}$−Ni1−$O4^{\#1}$	106.26(6)
O2−C11	1.255(3)	N3−Ni1−$O4^{\#2}$	154.82(6)
O3−C16	1.268(2)	$O4^{\#1}$−Ni1−$O4^{\#2}$	89.68(8)
O4−C16	1.266(2)	O1−Ni2−$O1^{\#4}$	180.00(7)
		O1−Ni2−$O5^{\#4}$	88.78(6)
		O1−Ni2−O5	91.22(6)
		$O5^{\#4}$−Ni2−O5	180.0
		O1−Ni2−$N1^{\#4}$	91.24(6)
		O5−Ni2−$N1^{\#4}$	92.78(7)
		O1−Ni2−N1	88.76(6)
		O5−Ni2−N1	87.22(7)
		$N1^{\#4}$−Ni2−N1	180.0
		O2−C11−O1	125.11(19)
		O4−C16−O3	118.90(18)

[a] Symmetry transformations to generate equivalent atoms: #1 $-x+1/2, y-3/2, -z+3/2$; #2 $x-1/2, y-3/2, z$; #3 $-x, y, -z+3/2$; #4 $-x+1/2, -y-3/2, -z+1$.

(25) Blatov, V. A.; Carlucci, L.; Ciani, G.; Proserpio, D. M. *CrystEngComm* **2004**, *6*, 378−395.
(26) Blatov, V. A.; Shevchenko, A. P.; Serezhkin, V. N. *J. Appl. Crystallogr.* **2000**, *33*, 1193.

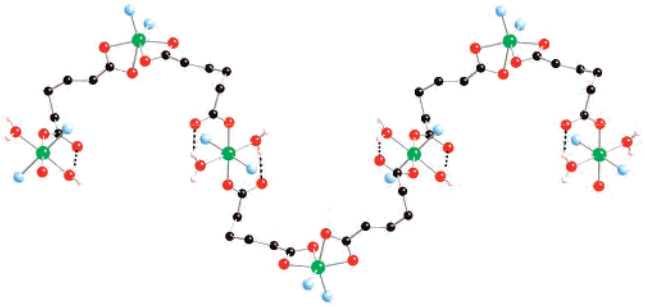

Figure 6. Single sinusoidal 1-D [Ni(adp)(H_2O)] ribbon in **2**. Intrachain hydrogen bonding is shown as dashed lines.

fashion. This adipate binding mode stands in contrast to that observed in the 1-D coordination polymer [Ni(adp)(H_2O)$_4$],[27] wherein the adipate ligands link neighboring Ni ions in a bis-monodentate bridging fashion. To accommodate this monodentate/chelating bridging mode, which is unprecedented to the best of our knowledge for the adipate ligand, the adipate dianions in **2** adopt a "hairpin" anti−gauche−gauche conformation (torsion angles 171.1, 54.0, and 55.0°). The chelating carboxylate terminus is situated at the anti conformation side of the aliphatic chain. Neutral sinusoidal 1-D [Ni(μ_2-adp)(H_2O)] ribbons propagate along the (1 0 1) direction of the crystal (Figure 6). The Ni1−Ni2 distance within these ribbons is 8.397(1) Å, shorter by ∼1.1 Å than the corresponding μ_2-adipate bridged Co−Co distance in **1**. This substantial decrease can be ascribed to the hairpin adipate conformation in **2**. The "wavelength" of the sinusoidal ribbon motifs is ∼ 21 Å, as determined by the second nearest-neighbor Ni1−Ni1 distance. Within each [Ni(μ_2-adp)(H_2O)] ribbon motif, the aquo ligands attached to Ni2 engage in hydrogen-bonding donation to the unligated adipate carboxylate oxygen atoms, thus stabilizing the monodenticity of the carboxylate subunit on each adipate ligand and preventing the bischelating binding mode seen in **1**. Adjacent [Ni(μ_2-adp)(H_2O)] ribbons are connected into a pseudo 2-D layer via hydrogen-bonding donation from the Ni2-bound aquo ligands to chelating carboxylate oxygen atoms bound to Ni1, as shown in Figure 7.

The ribbon motifs are covalently connected into the full 3-D crystal structure of **2** by means of infinite [Ni(dpa)] chains, which course in a perpendicular direction. These structural subunits form via the connection of Ni1 and Ni2 atoms in different [Ni(adp)(H_2O)] ribbons through tethering dpa moieties. Because of the alternating cis and trans orientations of dpa nitrogen donors at Ni1 and Ni2, respectively, these infinite [Ni(dpa)] chains adopt a zigzag-style arrangement (Figure 8). The Ni−Ni contact distance within this second type of chain motif in **2** is 11.482(1) Å; the "wavelength" of the zigzag repeat pattern is nearly 35 Å.

The covalent cross-linking of the [Ni(μ_2-adp)(H_2O)] ribbons and [Ni(dpa)] chains results in a 3-D network based on the linking of tetrahedral 4-connected nodes (at Ni1, caused by cis dpa coordination) and square planar 4-connected nodes (at Ni1, caused by trans dpa coordination), affording a cooperite-type (pts)[24] structure with $4^2 8^4$ topology.[28] The long vertex symbols for the 4-connected Ni1 and Ni2 nodes are $4.4.8_2.8_2.8_8.8_8$ and $4.4.8_7.8_7.8_7.8_7$. The pts networks in **2** are 3-fold interpenetrated (Figure 9), representing the highest level of interpenetration observed for this structure type to date; the FIV[25] relating the Class Ia translation-only interpenetrated networks is (0,1,0) with a translation distance of 9.36 Å, as calculated by TOPOS.[26] The 3-D covalent connectivity of **2** is augmented by hydrogen bonding between the central N−H unit of the two distinct dpa ligands and carboxylate oxygen atoms, in

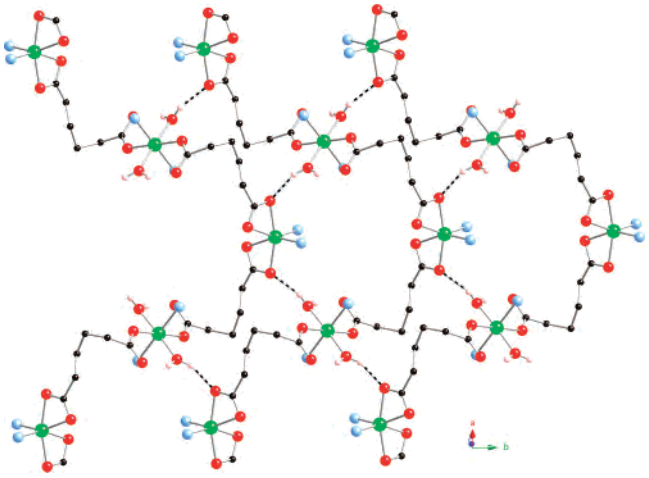

Figure 7. Pseudo-2-D layer composed of hydrogen-bonded 1-D [Ni(adp)(H_2O)] ribbons in **2**. Interribbon hydrogen bonding is shown as dashed lines.

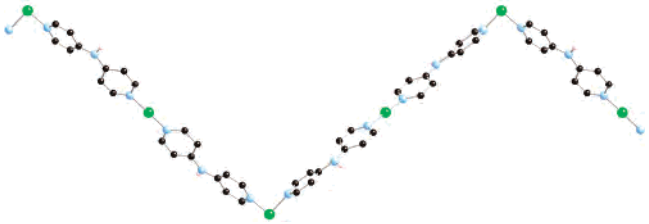

Figure 8. Zigzag 1-D [Ni(dpa)] chain motif in **2**, highlighting alternating cis and trans dpa coordination.

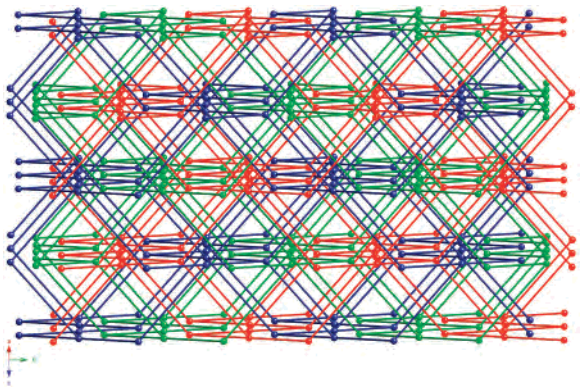

Figure 9. Framework perspective of the unprecedented triply interpenetrated pts net 3-D structure of **2**. Each independent framework is depicted in a different color. Ni atoms are shown as spheres, while the rods represent the adp and dpa ligands.

(27) Bakalbassis, E. G.; Korabik, M.; Michailides, A.; Mrozinski, J.; Raptopoulou, C.; Skoulika, S.; Terzis, A.; Tsaousis, D. *Dalton Trans.* **2001**, 850−857.

(28) Carlucci, L.; Ciani, G.; Gudenberg, D. W. v.; Proserpio, D. M. *New J. Chem.* **1999**, *23*, 397−401.

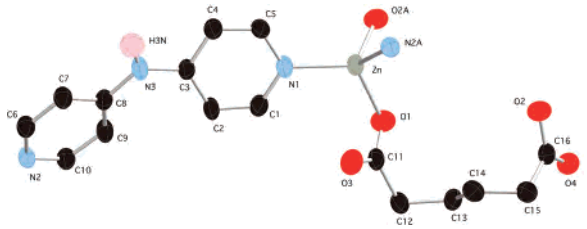

Figure 10. Expanded asymmetric unit of **3** with thermal ellipsoids at 50% probability. Most hydrogen atoms have been omitted for clarity.

Table 5. Selected Bond Distances (Å) and Angles (deg) for **3**

Zn1−O1	1.950(2)	O1−Zn1−O2	97.73(10)
Zn1−O2	1.969(2)	O1−Zn1−N2	110.81(10)
Zn1−N2	2.030(2)	O2−Zn1−N2	105.60(10)
Zn1−N1	2.037(2)	O1−Zn1−N1	115.03(10)
O1−C11	1.270(4)	O2−Zn1−N1	112.98(10)
O2−C16	1.292(4)	N2−Zn1−N1	113.30(10)
O3−C11	1.232(4)	O3−C11−O1	123.4(3)
O4−C16	1.234(4)	O4−C16−O2	122.3(3)

addition to $\pi-\pi$ stacking interactions between neighboring dpa pyridyl rings (centroid-to-centroid distance = 3.754(1) Å with an interring dihedral angle of 20.2°). Supramolecular hydrogen-bonding distances and angles for **2** are given in Table 3.

Structural Description of [Zn(adp)(dpa)]·H_2O (3). Single-crystal X-ray diffraction revealed that **3** contains an asymmetric unit (Figure 10) consisting of one zinc atom, one adipate ligand in an S-shaped gauche−anti−gauche conformation (torsion angles of 61.6, 175.3, and 56.9°), one dpa ligand, and one water molecule of crystallization hydrogen bonded to the secondary amine group of the dpa ligand. In contrast to the octahedral coordination geometries at the metal atoms in **1** and **2**, Zn manifests a [ZnO_2N_2] slightly distorted tetrahedral coordination sphere with bond angles ranging between 97.7 and 115.0°. The Zn−N bond lengths are slightly longer than the Zn−O bond lengths. The adp ligands adopt a bismonodentate bisbridging binding mode, with the ligated carboxylate oxygen atoms exhibiting C−O bond distances ~0.06 Å longer than the unligated carboxylate oxygen atoms. Selected bond distance and angle information for **3** is given in Table 5.

In contrast with **1** and **2**, where the adipate ligands serve to propagate the extended crystal structures in 2-D and 1-D, respectively, two adipate anions in **3** simply connect neighboring Zn atoms to form neutral [$Zn_2(adp)_2$] bimetallic kernels bearing 18-membered $(ZnOC_6O)_2$ rings (Figure 11). The Zn−Zn distance across the bimetallic unit is 5.932(1) Å. Each [$Zn_2(adp)_2$] kernel connects to four others through tethering dpa ligands, thereby forming infinite 2-D layers (Figure 12). The through-ligand Zn−Zn distance through the dpa tethers is 11.541(1) Å. If each Zn atom is considered as a 3-connected node, with the double adipate bridge treated as a single connection, a (6,3) graphitic layer can be invoked. Covalent connectivity within the layer motif is augmented by weak C−H···O interactions between the pyridyl rings and unligated adipate carboxylate oxygen atoms (C1···O3 = 3.192 Å, C5···O4 = 3.091 Å). Water molecules of crystallization lie within the layers, anchored into place via hydrogen-bonding acceptance from the central N−H units

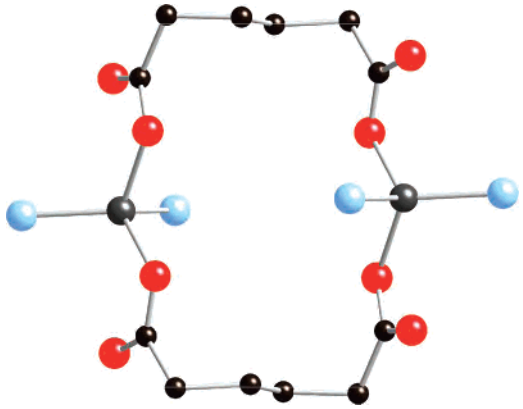

Figure 11. [$Zn_2(adp)_2$] 18-membered ring bimetallic kernel in **3**. Nitrogen atoms bound to Zn are also shown.

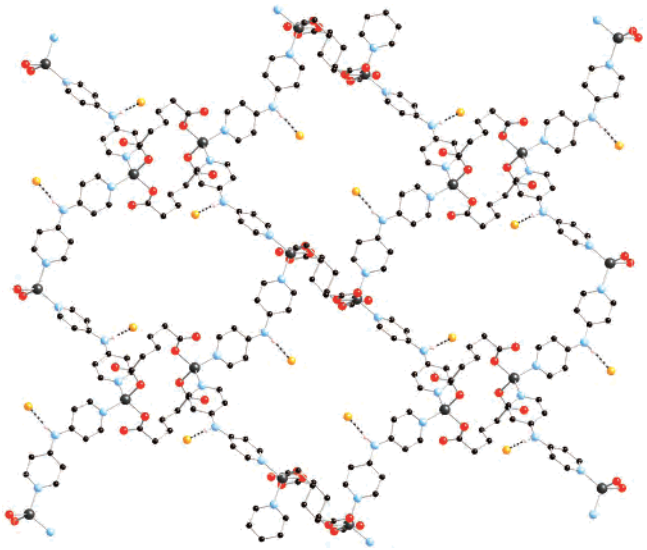

Figure 12. A single {[Zn(adp)(dpa)]·H_2O} 2-D layer in **3**. Water molecules of crystallization are shown in orange. Hydrogen-bonding interactions are depicted as dashed lines.

of the dpa moieties (see Table 3 for supramolecular metrical parameters). Removal of the uncoordinated water molecules from the unit cell of **3** reveals small incipient void spaces (1.9% of the cell volume as calculated by PLATON).

As seen in Figure 13, the full pseudo-3-D crystal structure of **3** consists of two sets of mutually inclined polycatenated[29] (2d + 2d → 3D) (6,3) graphitic [Zn(adp)(dpa)] layers, similar to the [Cu_2(pyrazine)$_3(SiF_6)$] prototype discovered by Zaworotko.[30] One set of layers (type A, in red) is oriented parallel to the (1 1 0) crystal plane, and the other (layer type B, in green) is parallel to (1 −1 0) plane. The angle subtended by the intersection of one layer A and one layer B is ~43.4°. The closest Zn−Zn distance between layers of the same type is 8.542(1) Å, while the corresponding Zn−Zn nearest approach between layers of different type is 7.287(1) Å. The [$Zn_2(adp)_2$] neutral bimetallic kernels from layers of type A slot into the open incipient void spaces in neighboring type B layers, assisted by hydrogen-bonding donation between

(29) Carlucci, L.; Ciani, G.; Proserpio, D. M. *Coord. Chem. Rev.* **2003**, *246*, 247−289.
(30) MacGillivray, L. R.; Subramanian, S.; Zaworotko, M. J. *J. Chem. Soc., Chem. Commun.* **1994**, 1325−1326.

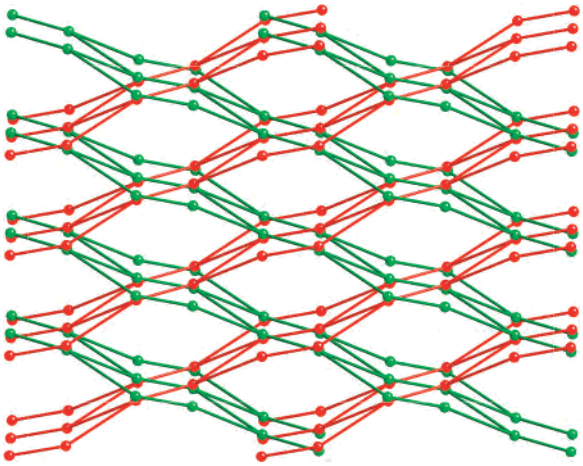

Figure 13. Framework view of mutually inclined polycatenated (6,3) layer motifs in **3**. Zn atoms are shown as spheres, while the organic tethers are drawn as rods.

the water molecules of crystallization within one layer and ligated (O2) and unligated (O3) adipate carboxylate oxygens belonging to adjacent layers. In addition, weak interlayer C−H···O interactions between dpa pyridine rings and unligated adipate oxygen atoms play a supplemental stabilizing role (C10···O4 distance = 3.143 Å). The structural pattern of **3** is unprecedented for organodiimine-tethered zinc dicarboxylates, standing in stark contrast to [Zn(adp)(4,4′-bpy)],[31] which crystallizes in a doubly interpenetrated pcu structure type similar to that of **1**.

Thermogravimetric Analysis. All new phases were subjected to thermogravimetric analysis to ascertain their thermal robustness. Compound **1** was thermally stable until ∼280 °C, whereupon it underwent decarboxylation (5.8% mass loss observed, 5.9% calculated for one molar equivalent of CO_2), followed by a subsequent 30.9% mass loss beginning at ∼350 °C and ending at ∼450 °C, roughly corresponding to the loss of one carboxylated and one decarboxylated adipate (32.6% predicted). Loss of all dpa ligands was complete by ∼680 °C (42.9% mass loss observed, 45.7% predicted). The final mass was consistent with the deposition of Co_3O_4 (21.9% mass remaining, 21.4% calculated). Compound **2** lost its coordinated water at ∼130 °C (5.1% mass loss observed, 4.6% calculated). Catastrophic degradation commenced at ∼330 °C (65.4% mass loss, 68.6% predicted for two dpa ligands, one adipate ligand, and decarboxylation of the other adipate ligand). At ∼590 °C, the remaining decarboxylated adipate was lost (13.5% mass loss, 12.7% predicted). The final mass remnant (19.0% of the original) correlated exactly with that calculated for NiO. Compound **3** underwent dehydration between 120 and 175 °C (5.7% mass loss, 4.5% predicted). Its mass remained stable until 240 °C, whereupon a series of mass losses ensued corresponding to elimination of organic fragments. The 34.3% mass remnant at 900 °C is roughly consistent with $Zn(CN)_2$ (29.4% calculated), a remnant seen previously upon thermolysis of other zinc coordination polymers with organoimine ligands.[32] TGA traces for **1**−**3** are shown in Figures S1−S3.

Dehydration/Rehydration Behavior of 3. To further probe the dehydration behavior of **3**, a sample was heated in air at 180 °C for 48 h. The powder XRD pattern of as-synthesized **3** is shown in Figure S4. Powder XRD revealed that a structural transformation to a new phase had occurred upon dehydration, which exhibited an orthorhombic unit cell with $a = 17.685(2)$ Å, $b = 21.161(1)$ Å, and $c = 16.691(3)$ Å (Figure S5). Unfortunately, this dehydrated phase was polycrystalline, precluding single-crystal structure determination. It is plausible that the adipate ligands adopt a different conformation in response to the loss of hydrogen bonding imparted by the water molecules of crystallization, resulting in structural reorganization. Immersion of the dehydrated material in water for 48 h regenerated the structure of **3** according to powder XRD (Figure S6). Reversible guest-induced crystal-to-crystal transformations have been reported in several other coordination polymer systems.[33] Attempts to fully structurally characterize the dehydrated orthorhombic phase are underway.

Magnetic Properties of 1. The magnetic susceptibility of **1** was measured as a function of temperature to probe any spin communication between carboxylate-bridged Co atoms. The value of the $\chi_m T$ product was 5.62 cm^3 K mol^{-1} Co_2 dimeric units at 300 K, roughly consistent with the value for two coupled $S = 3/2$ Co^{2+} ions (6.00 cm^3 K mol^{-1}). The $\chi_m T$ product decreased only slightly until 100 K (Figure 14), whereupon a more rapid decrease was observed, with a value of 1.00 cm^3 K mol^{-1} at 2 K. This diminution in $\chi_m T$ is consistent with antiferromagnetic coupling across the binuclear kernels in **1**, although single-ion anisotropy (D parameter) resulting from the distorted octahedral coordination about Co or spin−orbit coupling cannot be ruled out. A plot of $1/\chi_m$ versus T revealed that the magnetic susceptibility of **1** follows the Curie−Weiss law ($\chi_m = C/T - \Theta$) between 100 and 300 K with a C value of 5.66 cm^3 K mol^{-1} and $\Theta = -3.3$ K, again indicative of antiferromagnetic coupling between Co centers in **1**. Similar weak antiferromagnetic coupling was observed in the previously reported related [Co(adp)(L)] (L = 1,2-di-4-pyridylethane, *trans*-1,2-di-4-pyridylethylene) phases.[12] Given the small negative value of Θ in **1**, any spin communication between more-remote Co atoms bridged by the bischelating adipate moieties or the tethering dpa ligands can be considered negligible.

Luminescent Properties of 3. In the solid state at room temperature, **3** exhibited blue-violet luminescence upon ultraviolet excitation ($\lambda = 250$ nm), displaying an emission spectrum with a broad feature centered at $\lambda_{max} \approx 350$ nm and an extensive tail protruding into visible wavelengths. Emission and excitation spectra for **3** are shown in Figure 15. Unligated dpa is also luminescent, showing a weak broad emission with $\lambda_{max} = 420$ nm at the same excitation wavelength. Therefore, by comparison with other zinc and

(31) Zheng, Y.-Q.; Ying, E.-B. *Polyhedron* **2005**, *24*, 397−406.

(32) Ouellette, W.; Hudson, B. S.; Zubieta, J. *Inorg. Chem.* **2007**, *46*, 4887−4904.

(33) Kitagawa, S.; Kitaura, R.; Noro, S. *Angew. Chem., Int. Ed.* **2004**, *43*, 2334−2375 and references therein.

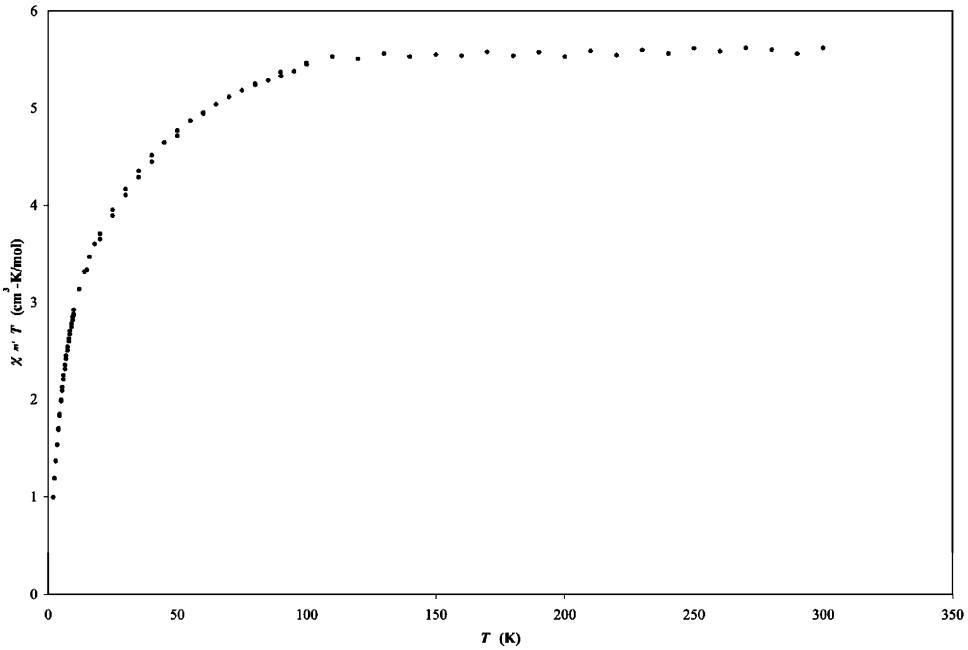

Figure 14. Plot of $\chi_m T$ vs T for **1**.

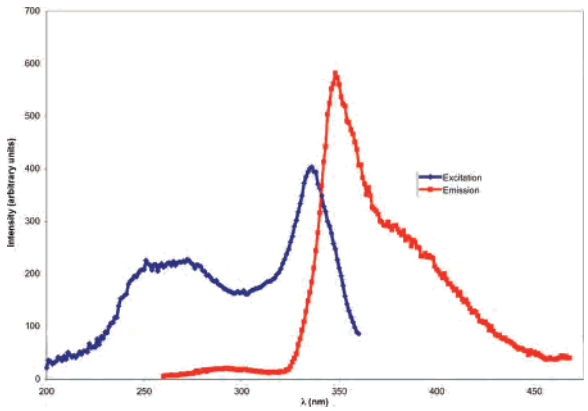

Figure 15. Solid-state excitation/emission spectrum of **3**.

cadmium dicarboxylate organodiimine coordination polymers,[34] the luminescent behavior of **3** is best rationalized by dpa ligand-centered $\pi \rightarrow \pi^*$ or $\pi \rightarrow$ n orbital transitions.

Conclusions

Hydrothermal synthesis has cleanly afforded three divalent metal coordination polymers incorporating both the kinked organodiimine 4,4′-dipyridylamine and the conformationally flexible adipate ligand. While the Co (**1**) and Ni (**2**) derivatives both display octahedral coordination geometry, the presence of coordinated water molecules in the latter provokes a shift from a doubly interpenetrated pcu topology in **1** to an unprecedented binodal triply interpenetrated pts morphology in **2**. Tetrahedral coordination in the Zn congener (**3**) promotes the formation of inclined polycatenated 2D → 3D graphite-like coordination polymer layers. All structures illustrate the capability of the adipate ligand to adopt energetically similar binding modes and conformations, wherein subtle variations can amplify and therefore assist in the development of the observed varied topologies and interpenetration or polycatenation. Hydrogen bonding and $\pi-\pi$ stacking supramolecular interactions imparted by the dpa ligand also play an important structure-directing role in the present case. Continued efforts to explore the construction of novel coordination polymers incorporating both 4,4′-dipyridylamine and flexible aliphatic dicarboxylate ligands are underway in our laboratory and will be reported in due course.

Acknowledgment. The authors gratefully acknowledge Michigan State University for financial support of this work. We are indebted to Troy E. Knight for acquisition of the fluorescence spectra. We thank Dr. Rui Huang for elemental analysis, Maxwell Braverman and Guilherme Cavichioli for experimental assistance, and Dr. Janice S. Pawloski (Grand Valley State University) for helpful discussions. M.R.M. thanks the MSU Introductory Chemistry Honors Program for his participation in this research. We thank one of the reviewers for very helpful suggestions.

Supporting Information Available: CIF files, TGA traces for **1**−**3**, and powder XRD patterns for as-synthesized, dehydrated, and rehydrated **3**. This material is available free of charge via the Internet at http://pubs.acs.org. Crystallographic data (excluding structure factors) for **1**−**3** have been deposited with the Cambridge Crystallographic Data Centre (nos. 636517−636519). Copies of the data can be obtained free of charge via the Internet at http://www.ccdc.cam.ac.uk/conts/retrieving.html or by post at CCDC, 12 Union Road, Cambridge CB2 1EZ, U.K. (fax: 44-1223336033; e-mail: deposit@ccdc.cam.ac.uk).

IC070291D

(34) (a) Tao, J.; Shi, J. X.; Tong, M. L.; Zhang, X. X.; Chen, X. M. *Inorg. Chem.* **2001**, *40*, 6328−6330. (b) Tao, J.; Tong, M. L.; Shi, J. X.; Chen, X. M.; Ng, S. W. *Chem. Commun.* **2000**, 2043−2044. (c) Dai, J. C.; Wu, X. T.; Fu, Z. Y.; Cui, C. P.; Hu, S. M.; Du, W. X.; Wu, L. M.; Zhang, H. H.; Sun, R. Q. *Inorg. Chem.* **2002**, *41*, 1391−1396. (d) Chen, W.; Wang, J. Y.; Chen, C.; Yue, Q.; Yuan, H. M.; Chen, J. S.; Wang, S. N. *Inorg. Chem.* **2003**, *42*, 944−946. (e) Hao, N.; Shen, E.; Li, Y. B.; Wang, E. B.; Hu, C. W.; Xu, L. *Eur. J. Inorg. Chem.* **2004**, 4102−4107.